Available online at www.sciencedirect.com
SCIENCE DIRECT
Acta Materialia 54 (2006) 3665–3672
Acta MATERIALIA
www.actamat-journals.com

# The role of carbon diffusion in ferrite on the kinetics of cooperative growth of pearlite: A multi-phase field study

Katsumi Nakajima [a], Markus Apel [b], Ingo Steinbach [b,*]

[a] JFE Steel Corporation, Steel Research Laboratory, 1 Kokan-cho, Fukuyama, Hiroshima 721-8510, Japan
[b] RWTH-Aachen, Access eV, Intzestrasse 5, D-52072 Aachen, Germany

Received 2 September 2005; received in revised form 8 February 2006; accepted 27 March 2006
Available online 22 June 2006

**Abstract**

Cooperative growth of pearlite is simulated for eutectoid steel using the multi-phase field method. The model considers diffusion of carbon not only in γ phase, but also in α phase. The lamellar spacing and growth velocity are estimated for different undercoolings and compared with experimental results from the literature and theoretical results from analytical models. The important finding of this work is that carbon diffusion in ferrite and growth of cementite from the ferrite increase the kinetics of the pearlitic transformation by a factor of four as compared to growth from austenite only, which is assumed by the classic Zener–Hillert model. This growth mode therefore must be considered to be the dominating growth mode and it explains at least some of the differences between experiment and theory, where diffusion in ferrite is excluded.


*Keywords:* Phase field models; Simulation; Pearlitic steels; Phase transformation kinetics; Microstructure

## 1. Introduction

The phase field method has proved to be a useful numerical tool to calculate the lamellar microstructure during eutectic solidification processes. In this paper, the method is applied to eutectoid transformation in the solid state. Analytical models of pearlite transformation and eutectic solidification are first reviewed and compared with each other.

Pearlite transformation is a well-known eutectoid transformation, where one parent phase decomposes into two solid phases simultaneously. It is similar to eutectic solidification, except for the phase state of the parent phase. The parent phase in the latter is liquid; in the former it is solid. Both transformations can lead to a lamellar microstructure. So far analytical models [1–3] have been suggested for the lamellar growth mode for either transformation. Three parameters are required to describe the formation of a lamellar structure, namely undercooling, lamellar spacing and growth velocity. Analytical models for both transformations differ in the thermal situation. While in the case of pearlitic growth the Zener–Hillert model [1,2] considers an isothermal situation, the Jackson–Hunt model [3] for eutectic solidification deals with directional solidification conditions. In the Zener–Hillert model, the growth velocity is free to adjust and undercooling is fixed. Jackson and Hunt applied the analytical solution from Ref. [2] to the growth conditions of eutectic growth in a temperature gradient, where the velocity is fixed by the growth condition and undercooling is free to adjust.

Concerning the velocity $v$ of cooperative growth in pearlite transformation, Zener and Hillert derived the following equation as a function of lamellar spacing:

$$v = (2D_\gamma/f^\alpha f^{\mathrm{cm}})\{(C_{\mathrm{e}}^{\gamma/\alpha} - C_{\mathrm{e}}^{\gamma/\mathrm{cm}})/(C^{\mathrm{cm}/\gamma} - C^{\alpha/\gamma})\} \times (1/\lambda)(1 - \lambda_0/\lambda) \quad (1)$$

where $D_\gamma$, $f^\alpha$ and $f^{\mathrm{cm}}$ represent carbon diffusion coefficient in γ phase ($\mathrm{cm}^2/\mathrm{s}$), volume fraction of α phase and volume fraction of cementite, respectively. $C^{\alpha/\gamma}$ and $C^{\mathrm{cm}/\gamma}$ represent

* Corresponding author. Tel.: +49 241 8098000; fax: +49 241 38578.
*E-mail address:* I.Steinbach@access.rwth-aachen.de (I. Steinbach).

1359-6454/$30.00 
doi:10.1016/j.actamat.2006.03.050

the carbon concentration in α phase and in cementite at the eutectoid transformation interface at a given undercooling, respectively. $C_e^{\gamma/\alpha}$ and $C_e^{\gamma/cm}$ represent the carbon concentration in γ phase in front of α phase and in front of cementite, respectively. The subscript e denotes equilibrium. $\lambda_0$ denotes the lamellar spacing where all energy is consumed for the formation of interfaces, i.e. $\lambda_0 = 2\sigma V_m/\Delta G$. Here $\sigma$, $V_m$ and $\Delta G$ represent surface energy (J/m$^2$), molar volume (m$^3$/mol) and change of total free energy (J/mol), respectively. If a criterion is assumed that a system transforms at maximum velocity, Eq. (1) reduces to Eq. (2) under $\lambda = 2\lambda_0$:

$$v = (D_v/2f^{\alpha}f^{cm})\{(C_e^{\gamma/\alpha} - C_e^{\gamma/cm})/(C^{cm/\gamma} - C^{\alpha/\gamma})\}(1/\lambda) \quad (2)$$

The term $(C_e^{\gamma/\alpha} - C_e^{\gamma/cm})/(C^{cm/\gamma} - C^{\alpha/\gamma})$ is proportional to the reciprocal lamellar spacing. Consequently velocity is approximately proportional to $1/\lambda^2$.

If the deviation of the actual transformation temperature from the eutectoid temperature is small, $\Delta G$ is expressed approximately as $\Delta H \times \Delta T/T_E$, using the latent heat of pearlite transformation ($\Delta H$) and the eutectoid temperature ($T_E$). The relationship between undercooling and lamellar spacing is given by Eq. (3) using $\lambda = 2\lambda_0$ and $\lambda_0 = 2\sigma V_m/\Delta G$:

$$\Delta T = 4\sigma T_E V_m/\Delta H(1/\lambda) \quad (3)$$

In the case of eutectic solidification, Jackson and Hunt [3] derived the following equation for lamellar growth:

$$\Delta T/m = Qv\lambda + a/\lambda \quad (4)$$

where $m$, $Q$ and $a$ are constants. If the criterion is assumed that a solid grows at minimum undercooling, which corresponds to the maximum growth criterion in pearlite transformation, Eq. (4) reduces to Eqs. (5) and (6):

$$\Delta T = 2ma(1/\lambda) \quad (5)$$

$$v = a/Q(1/\lambda^2) \quad (6)$$

Figs. 1 and 2 show the relationship between lamellar spacing and undercooling and between lamellar spacing and growth velocity. It is revealed that both pearlite transformation and eutectic solidification have similar relationships among the three parameters. Here two important things must be kept in mind. One is that these analytical models are based on the diffusion-controlled mode and the other is that they consider diffusion in the parent phase only.

Fig. 3 shows a schematic phase diagram of the Fe–C system related to the pearlite transformation. Here an undercooling of 50 K is supposed as an example. Dotted lines mean extrapolated lines of $A_{e3}$, $A_{cm}$ and solubility line of α phase in γ phase. It is obvious that during isothermal transformation of pearlite with constant undercooling, there are concentration differences in both γ phase and α phase. These concentration differences create a driving force for diffusion in both phases as illustrated in Fig. 4. It is likely that diffusion in the α phase has a considerable influence on transformation behavior because the carbon diffusion coefficient in α phase is much larger than that in the γ phase. Therefore diffusion in both phases should be taken into consideration in order to simulate pearlite transformation. The importance of carbon diffusion in ferrite was first pointed out by Onsager in 1948 [4], and Fisher [5] calculated in 1959 a growth rate 7 times faster by this transformation path than by diffusion in austenite only. However, since the diffusion data used by Fisher were doubted [2] and in an experimental study by Mehl and Hagel [6] no evidence was found for a tapered form of the cementite behind the growth front, which should be characteristic for this transformation path, the possibility of the transformation path by cementite growth from ferrite was disregarded in further studies. As an alternative, grain boundary diffusion was proposed to explain the discrepancy between theory and experiment [7].

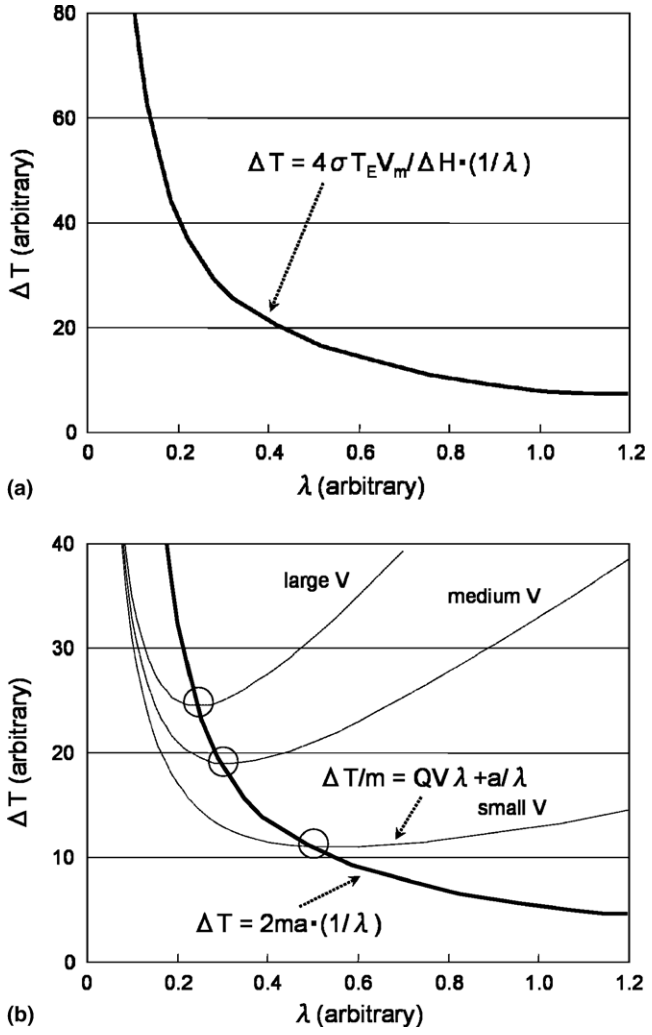


Fig. 1. Relationship between spacing and undercooling according to analytical models.

The purposes of this study are to investigate complex cooperative growth of pearlite transformation by a multi-phase field model and to clarify the influence of diffusion

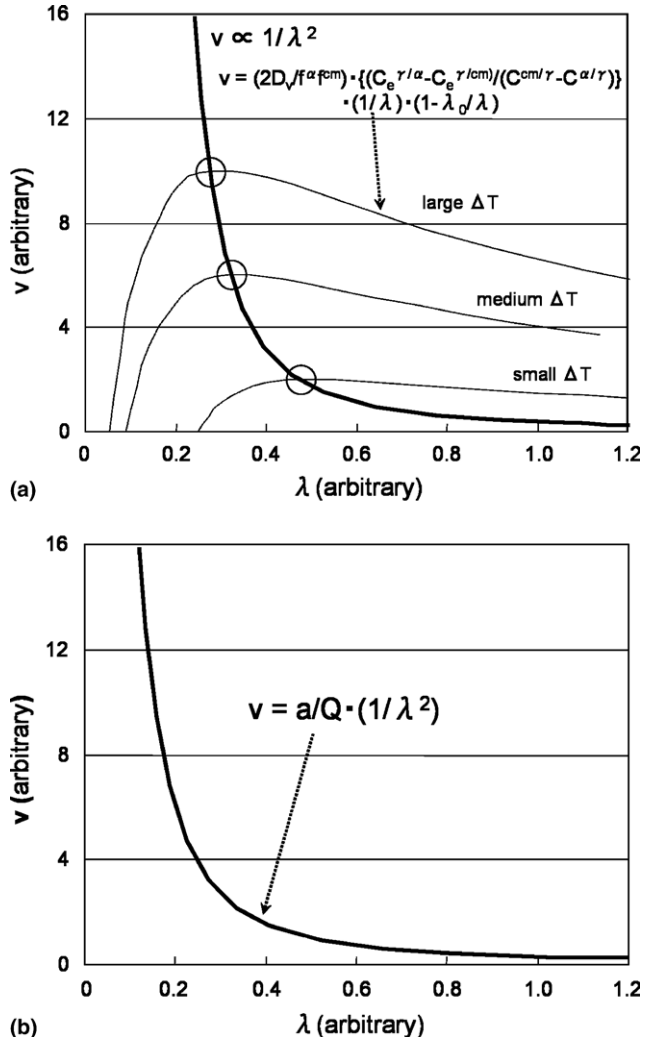


Fig. 2. Relationship between spacing and growth velocity according to analytical model.

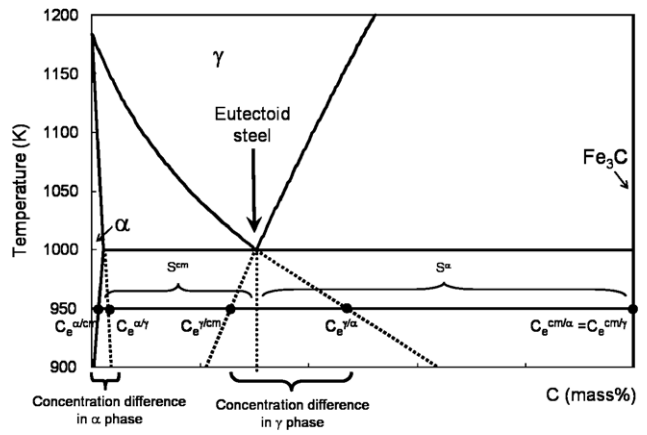


Fig. 3. Schematic Fe–C system related to pearlite transformation.

in α phase. Regarding eutectic solidification, phase field simulation has been performed for a variety of systems [8–10]. However, so far, phase field simulations have not

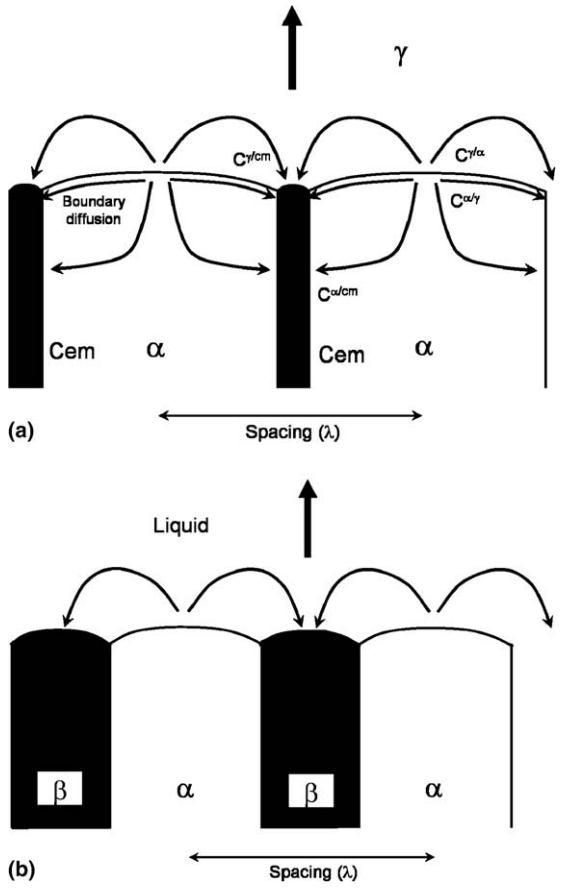


Fig. 4. Possible diffusion paths during transformation.

yet been reported for pearlite transformation. Several factors make the simulation in the case of cooperative growth during pearlite transformation complex. The lamellar spacing in pearlite is usually smaller than that in eutectic solidification. Typical undercooling of the transformation front due to curvature therefore is of the order of 10–50 K depending on the transformation condition, more than a factor of 10 higher than during solidification under typical casting conditions. This undercooling has to be balanced by solutal supersaturation or thermodynamic driving force acting on the interface to reach a vanishing net driving force with vanishing kinetic undercooling (diffusion-controlled transformation mode). As curvature undercooling and solutal supersaturation are both subject to numerical fluctuations, instabilities arise if the amplitude of the fluctuations exceeds the time-averaged net driving force. At present this problem can only be controlled by selecting an appropriate value of the interface mobility (see below). A further problem is the large difference in carbon content between the cementite phase and ferrite or austenite, which causes a disparity in the interplay between diffusion and growth of both sides of the interface. All these factors hamper the numerical stability of the interface. An implicit solution scheme to tackle these problems at present is not available due to the high nonlinearity of the coupled phase field/diffusion problem.

## 2. Multi-phase field model

The multi-phase field model is an extension of basic phase field concepts to the interactions of multiple phases [11]. We give a brief description of the basic equations. Considering a system of $N$ phases, a set of field variables $\Phi_i$ ($i = 1, \ldots, N$) is introduced to describe the distribution of each phase in time and space. In the bulk of one phase $i$, $\Phi_i$ is equal to 1. Within an interface between phase $i$ and $j$, $\Phi_i + \Phi_j = 1$ ($\Phi_i < 1$, $\Phi_j < 1$) holds. In general, the following constraint must be fulfilled everywhere:

$$\sum \Phi_i = 1 \tag{7}$$

The microstructure evolves according to a decrease of total free energy. By using thermodynamic principles, we derive a set of multi-phase field equations [11]. In the case of a double obstacle potential, the equations are as follows:

$$\mathrm{d}\Phi_i/\mathrm{d}t = \sum \mu_{ij}[\sigma_{ij}\{\Phi_j\Delta\Phi_i - \Phi_i\Delta\Phi_j + \pi^2/(2\eta^2) \times (\Phi_i - \Phi_j)\} + \pi/\eta\sqrt{\Phi_i\Phi_j}\Delta G_{ij}] \tag{8}$$

for each phase field parameter $\Phi_i$, where $\eta$, $\sigma_{ij}$, $\mu_{ij}$ and $\Delta G_{ij}$ represent interface width (cm), surface energy (J/cm$^2$), interface mobility (cm$^4$/J s) and free energy difference of two interacting phases $i$ and $j$ (J/cm$^3$), respectively. We consider only the isotropic case and mobilities and surface energies are identical for any $i$/$j$ interface.

The equation consists of two terms. The first represents interface curvature; the latter represents the thermodynamic driving force. In our simulation, the thermodynamic driving force $\Delta G_{ij}$ for each calculation step is calculated using the carbon concentration $c_i$ from the previous calculation step as follows:

$$\Delta G_{ij} = \Delta S_{ij}(T^r + m_{ij}(c_i - c_i^r)\cdot T) \tag{9}$$

where $\Delta S_{ij}$, $T^r$, $m_{ij}$ and $c_i^r$ represent transformation entropy (J/K cm$^3$), reference temperature (K), slope of a corresponding line in phase diagram (slope of tangent given at a reference point) and the concentration at a reference temperature, respectively.

In the case of a single solute component, the diffusion equation for the overall concentration $c$ is expressed as follows [12,13]:

$$\mathrm{d}c/\mathrm{d}t = \nabla\cdot\sum \Phi_i D_i \nabla c_i = \nabla\cdot\left\{\sum \Phi_i D_i \nabla(k_{ir}c)/\left(\sum \Phi_j k_{jr}\right)\right\} \tag{10}$$

where $D_i$, $c_i$ and $k_{ir}$ represent diffusion coefficient in phase $i$, concentration in phase $i$ and concentration ratio between phase $i$ and $r$, respectively. This equation corresponds to the standard Ficks diffusion equation except for the interface region. Within the interface region, we define weighted fluxes of each component in each phase as seen in Eq. (11), which defines total concentration as a sum over phase concentrations $c_i$. Eq. (12) denotes the concentration ratio between interacting phases, which is calculated by ThermoCalc according to the parallel tangent construction under the constraint of fixed phase fractions $\Phi_i$:

$$c = \sum \Phi_i c_i \tag{11}$$

$$c_i = k_{ir}c_r \tag{12}$$

Phase field equations and diffusion equation are solved explicitly by the finite difference method using Micress® software [14].

The material applied for simulation is eutectoid steel (Fe, 0.77 mass%). We focus in this study on cooperative growth; nucleation is not treated. Initial lamellae are set and their spacing is varied from 0.1 to 1.0 μm. Undercooling is set to values of 10, 30 and 50 K. We consider two cases, namely single diffusion path in γ phase and double diffusion paths in both γ and α phases. As shown in Fig. 5, surface energy is fixed as 1.0 J/m$^2$ for all interfaces. Diffusion data are based on the literature [15]. Cementite is treated as stoichiometric. The most difficult task is to adjust the interface mobility of the phase field to ensure a diffusion-controlled transformation mode. As the thin interface correction scheme developed by Karma [16] is not yet worked out for finite diffusion in both components, interface mobility was chosen as high as possible but still avoiding instabilities of the interface. The mobilities used for the γ/α and the γ/Cem interface are two orders of magnitude higher than the values for interface mobilities in the mixed-mode transformation model of Krielaart and Van der Zwaag [17]; thus they can be used to approximate the diffusion-controlled mode. The maximum allowable value for the α/Cem mobility is three orders of magnitude smaller due to the instabilities arising from the large difference in equilibrium content of carbon between these two phases. The difficulty in selecting an appropriate interface mobility spoils the quantitative comparison of the simulation results with both theory and experiment. However, since the values were kept similar in all simulations, the difference in transformation mode, including or neglecting diffusion in ferrite, can clearly be deduced from the simulations. Earlier it was demonstrated by direct comparison of phase field calculations, using Micress®, with the commercial code Dictra that the diffusion-controlled transformation mode can be reproduced quantitatively in close to equilibrium situations [18].

| Phase diagram | | | ThermoCalc coupling |
|---|---|---|---|
| Interface properties | surface energy | σ | 1.0 J/m² (all interfaces) |
| | mobility | γ / α<br>γ / Cem<br>α / Cem | 5.0×10⁻⁵ – 1.0×10⁻⁴ cm⁴/Js<br>9.0×10⁻⁵ – 2.0×10⁻⁴ cm⁴/Js<br>9.0×10⁻⁸ – 5.0×10⁻⁷ cm⁴/Js |
| Diffusion | Carbon | γ | $D_0$=1.5×10⁻⁵ m²/s, Q=142.1 kJ/mol |
| | | α | $D_0$=2.2×10⁻⁴ m²/s, Q=122.5 kJ/mol |
| | | Cem | stoichiometry |

Fig. 5. Data used in simulations. Diffusion data from Ref. [16].

## 3. Results and discussion

### 3.1. Influence of spacing on lamellar formation

As shown in Fig. 2, the analytical model reviewed above revealed the dependence of the velocity of cooperative growth upon lamellar spacing in pearlite transformation. This means that the growth velocity cannot be determined uniquely at a given undercooling condition, but there is a range of possible spacings. At first we investigated the selection of lamellar spacing by using our multi-phase field model in order to verify this fundamental behavior. Representative results are shown in Figs. 6 and 7. Each figure exhibits the microstructure and its carbon concentration field after 2.8 s of growth, respectively. Undercooling is 30 K and diffusion is considered only in γ phase. The simulation starts with two seeds of cementite in a ferrite layer at the bottom of the calculation domain. Initial concentrations were set to the equilibrium values. The initial transient to steady-state growth results in a small dip in the cementite structure, which has no physical meaning. Similar behavior was found for all undercooling conditions and diffusion paths. From left to right, initial lamellar spacings are 0.15, 0.25 and 0.4 μm, respectively. As seen in these figures, in the case of the smallest spacing, which has the largest curvature at the transformation interface, the α phase overgrows cementite and a lamellar structure cannot evolve. Medium spacing exhibits the highest growth velocity (evaluated from the position of the pearlitic front and the time). It is obvious that the growth velocity decreases with increasing spacing, although the carbon concentration difference in the γ phase, which drives the diffusion from α phase to cementite through the γ phase, increases ahead of the transformation interface. The velocity of cooperative growth is determined by the combination of two factors. One is the diffusion distance from α phase to cementite where the shorter distance promotes a higher growth velocity. The other is curvature effect where a higher curvature slows down the growth velocity because it reduces the carbon concentration difference according to the Gibbs–Thomson effect.

The results of the phase field simulations for undercoolings of 30 and 50 K are plotted as square symbols in Fig. 8. The cross indicates a lamellar structure not being stable for this condition. Due to the high computational cost of the simulations only a limited number of calculations per case were possible. This seems, however, sufficient to prove the overall trend. From investigations on eutectic growth [19] it is also well known that a whole band of growth states is possible and the selection of the actual growth state depends on the history of the system. Because the focus of this work lies on the comparison of the growth modes with and without diffusion in ferrite, we do not attempt to find the absolute maximum of growth speed.

The solid lines in Fig. 8 represent Eq. (1) based on the Zener–Hillert model for undercoolings of 30 and 50 K. In this model, diffusion-controlled mode is assumed and diffusion is considered only in γ phase. The simulation results indicate a similar dependence of growth velocity

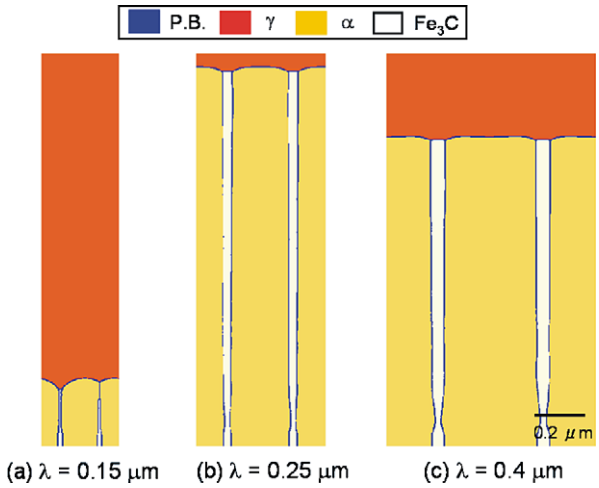


Fig. 6. Comparison of microstructures at time of 2.7 s for different spacings in the case of diffusion only in γ phase and $\Delta T = 30$ K.

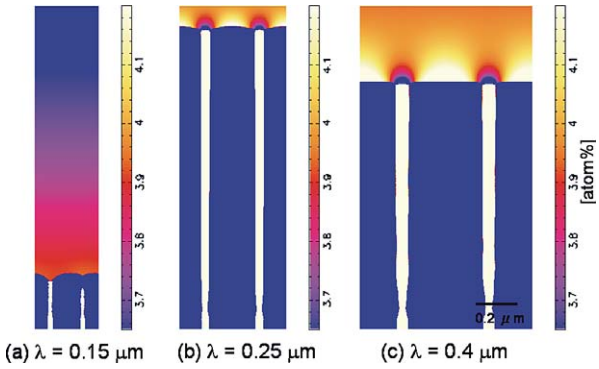


Fig. 7. Comparison of carbon concentration fields at time of 2.7 s for different spacings in the case of diffusion only in γ phase and $\Delta T = 30$ K.

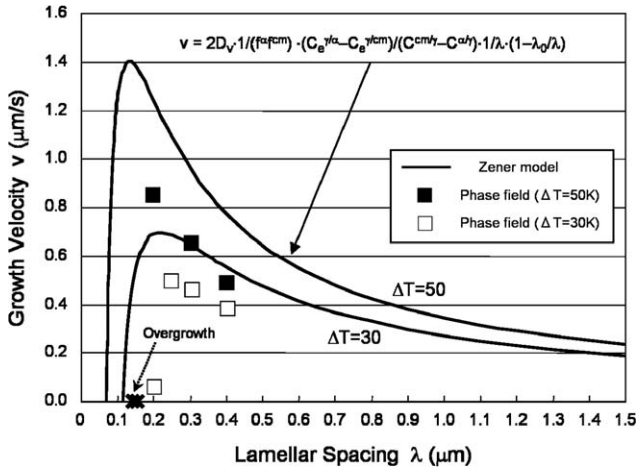


Fig. 8. Dependence of growth velocity upon spacing in the case of diffusion only in γ phase.

on lamellar spacing as the Zener–Hillert model. However, the growth velocity in the simulation always shows smaller values than the model. This difference is attributed to the value of mobility. While the analytical model is based on an infinite mobility, a finite mobility is used in the phase field simulations, which creates energy loss due to interface friction.

Fig. 9 shows the relationship between transformation temperature and reciprocal lamellar spacing. All experimental results are quoted from Ridley's summary [20] based on literature data [21–24]. They indicate an almost linear relationship except for the data at low temperatures. Simulation results are plotted by adopting the lamellar spacing which gives the maximum growth velocity for each undercooling, and they show a similar trend. However, the calculated values are smaller than the experimental observations. This discrepancy can be explained by two reasons. The first reason is the value of the surface energy, because the slope of the line depends on surface energy as recognized from Eq. (3). From a fit to the experimental data, the surface energy $\sigma$ is determined to be 0.94 J/m$^2$ using $\Delta H/V_m = 6.07 \times 10^8$ J/m$^3$ [25]. In our simulations, 1.0 J/m$^2$ was set for $\sigma$, which causes a smaller slope according to the analytical prediction. The difference in surface energy evokes about 30% of the deviations between experiment and simulation. The second reason again is the finite mobility used in the simulation. Other uncertainties like diffusion coefficients or the neglected effects of transformation strain and strain due to inhomogeneous carbon distribution will affect the agreement between the transformation kinetics in the simulation and reality. The treatment of diffusion in ferrite, as described below, is only one step towards fully understanding the pearlitic transformation.

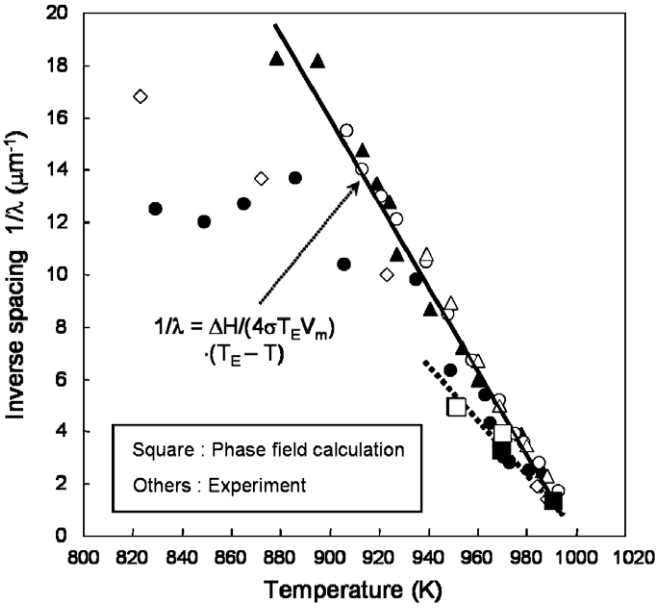


Fig. 9. Relationship between temperature and spacing.

### 3.2. Influence of the diffusion in α phase on the behavior of cooperative growth

So far analytical models of cooperative growth of pearlite have not considered the diffusion in the α phase. It is not clear a priori how the diffusion in the α phase influences the behavior of cooperative growth in pearlite. We executed simulations with and without diffusion in the α phase keeping all other conditions constant. Figs. 10 and 11 show typical results for a microstructure and its carbon concentration field, respectively. The left picture shows a snapshot of the lamellar structure at 0.58 s for the case of diffusion in both γ and α phases. The simulated structure after 2.2 s of growth shown in the right picture considers the diffusion only in the γ phase. Undercooling is set to 30 K and the initial lamellar spacing is 0.3 μm. The case of diffusion in both γ and α phases shows a growth velocity roughly four times higher than that of diffusion in austenite only, as seen in Fig. 10. Two differences in microstructure were found

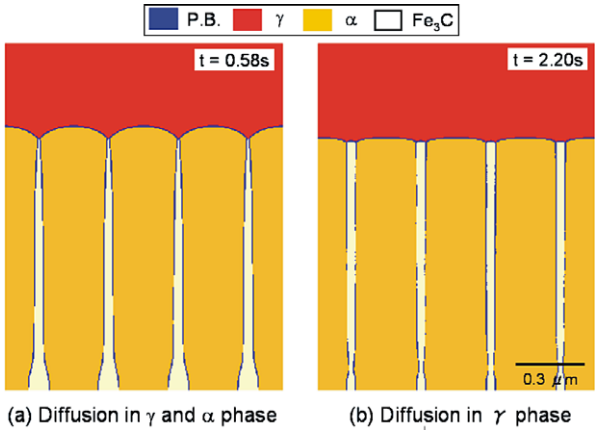


Fig. 10. Comparison of microstructures calculated with different diffusion paths in the case of $\Delta T = 30$ K and $\lambda = 0.3$ μm. Note that the time of the snapshot differs about by a factor of 4.

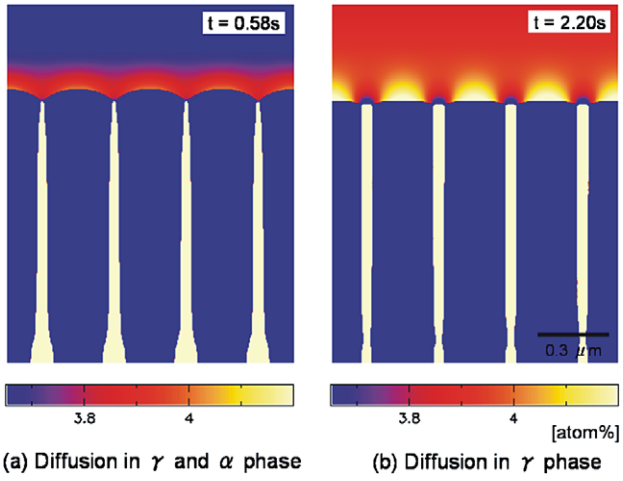


Fig. 11. Comparison of carbon concentration fields calculated for different diffusion paths in case of $\Delta T = 30$ K and $\lambda = 0.3$ μm.

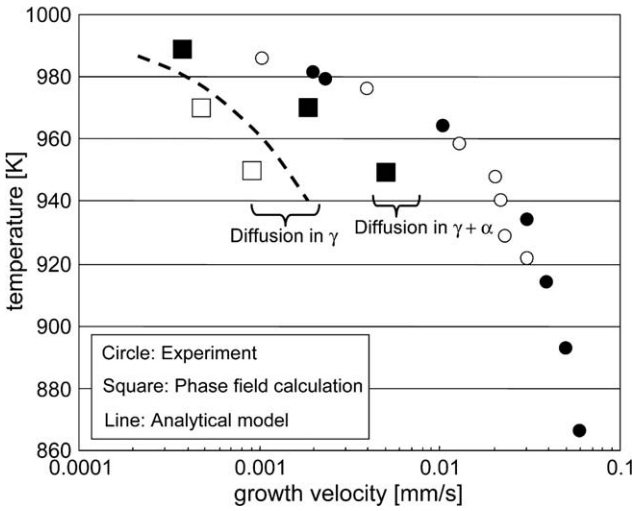


Fig. 12. Dependence of growth velocity upon temperature.

between these two pictures. The structure obtained for double diffusion path has always a larger curvature, which creates a smaller concentration difference of carbon in the γ phase ahead of the transformation as compared to the structure obtained for diffusion in γ only. A difference in the shape of cementite is also noted. In the left picture, lamellae are growing thicker into the α phase behind the eutectoid transformation front until the final cementite fraction is reached, because carbon is also supplied by the diffusion through the α phase. It is obvious that in the case of diffusion in both γ and α phases, the diffusion in α phase plays a dominant role for the kinetics of cooperative growth.

Fig. 12 plots simulation results of growth velocity against transformation temperature in addition to experimental results [22,26]. Each square symbol represents the maximum velocity calculated for each condition. The line is calculated using the Zener–Hillert model considering diffusion in the γ phase only.

In the case of diffusion only in the γ phase, phase field simulation and analytical model show similar behavior, although the phase field simulations do not reach the velocities predicted by the model. The simulation with the double diffusion paths in both γ and α phases exhibits a larger growth velocity than that with diffusion in the γ phase only, as mentioned above. However, the calculated velocities still do not fully explain the experimental values. Therefore also the influence of transformation strain, strain due to inhomogeneous carbon concentration and the influence of grain boundary diffusion on the transformation kinetics should be investigated in the future.

## 4. Conclusion

The evolution of a lamellar structure in the cooperative growth of pearlite in eutectoid steel was simulated for undercoolings of 10, 30 and 50 K, using the multi-phase field method. The simulation results show a similar dependence of growth velocity upon lamellar spacing as the Zener–Hillert model, although the absolute velocity in the simulations is always smaller because of the finite interface mobility in the simulation. A linear relationship between the transformation temperature and reciprocal spacing was found in the simulation results and experimental data. It was revealed that during growth the cementite shows a tapered profile when growing thicker from the ferrite, as proposed first by Onsager and Fisher [4,5]. This gives clear evidence that diffusion in α phase has a considerable influence on the kinetics of cooperative growth. Simulations with diffusion in both γ and α phases show a velocity four times larger than that with the diffusion only in γ phase. The strength of this effect comes from the high diffusivity of carbon in ferrite compared to austenite and from the large ratio of the ferrite/cementite interface area compared to the austenite/cementite interface area. Although there is some uncertainty in both the physical value of the interface mobility and the diffusion data, we conclude that diffusion in ferrite has a significant impact on the kinetics of pearlite transformation and that growth of cementite from the supersaturated ferrite is an important, if not the dominating transformation mode in pearlitic transformation of low-carbon steel.

## Acknowledgements

The authors thank Prof. M. Hillert for helpful discussions, Dr. B. Böttger and P. Schaffnit for their support in handling the phase field code and the JFE Steel corporation, Steel Research Laboratory under the management of Dr. Hosoya for financing this study.

## References

[1] Zener C. Trans AIME 1947;167:550.
[2] Hillert M. Jernkont Ann 1957;141:757–89.
[3] Jackson KA, Hunt JD. Trans Metall Soc AIME 1966;236:1129–42.
[4] Onsager L. Discussion. In: Cornell conference on solid state. August 1948 as cited in Ref. [2].
[5] Fisher JC. Thermodynamics in physical metallurgy. Cleveland (OH): ASM; 1950. p. 201–41.
[6] Mehl RF, Hagel WC. Prog Metal Phys 1956;6:74.
[7] Hillert M. Metall Trans 1972;3:2729–41.
[8] Karma A, Sarkissian A. Metall Mater Trans A 1996;27:635–56.
[9] Apel M, Boettger B, Diepers HJ, Steinbach I. J Cryst Growth 2002;237–239:154–8.
[10] Kim SG, Kim WT, Suzuki T, Ode M. J Cryst Growth 2004;261:135–58.
[11] Steinbach I, Pezzolla F, Nestler B, Seesselberg M, Prieler R, Schmitz GJ, et al. Physica D 1996;94:135–47.
[12] Tiaden J, Nestler B, Diepers HJ, Steinbach I. Physica D 1998;115:73–86.
[13] Eiken J, Böttger B, Steinbach I. Phys Rev E [in press].
[14] www.micress.de.
[15] Handbook of chemistry and physics. Boca Raton (FL): CRC Press; 1989.
[16] Karma A. Phys Rev Lett 2001;87:115701-1-4.
[17] Krielaart GP, van der Zwaag S. J Mater Sci 2001;36:519.
[18] Grafe U, Böttger B, Tiaden J, Fries SG. Scripta Mater 2000;42:1179–86.

[19] Kassner K, Misbah C, Baumann R. Phys Rev E 1995;51:2751–3.
[20] Ridley N. In: Marder AR, Goldstein JI, editors. Phase transformations in ferrous alloys. TMS-AIME; 1984. p. 201–36.
[21] Verhoeven JD, Pearson DD. Metall Trans A 1984;15:1047–54.
[22] Brown D, Ridley N. J Iron Steel Inst 1969;207:1232–40.
[23] Cheetham D, Ridley N. J Iron Steel Inst 1973;211:648–52.
[24] Bolling GF, Richman RH. Metall Trans 1970;1:2095–104.
[25] Kramer JJ, Pound GM, Mehl RF. Acta Metall 1958;6:763–71.
[26] Frye JH, Stansbury EE, McElroy DL. Trans AIME 1942;150: 185–207.